



ISSN: 2230-9926

Available online at <http://www.journalijdr.com>

IJDR

International Journal of Development Research

Vol. 11, Issue, 01, pp. 43318-43321, January, 2021

<https://doi.org/10.37118/ijdr.20799.01.2021>



RESEARCH ARTICLE

OPEN ACCESS

THERMAL DECOMPOSITION OF LANTHANUM NITRATE HEXAHYDRATE $\text{La}(\text{NO}_3)_3 \cdot 6\text{H}_2\text{O}$

*Hector Marcell Guerreiro, Petr Melnikov, Igor Arkhangelsky, Lincoln Carlos Silva de Oliveira, Gabriel Augusto Wandekoken and Valter Aragão do Nascimento

Universidade Federal de Mato Grosso do Sul–UFMS–Cidade Universitária, CEP:79080-190–
Campo Grande, MS- Brasil

ARTICLE INFO

Article History:

Received 17th October, 2020

Received in revised form

22nd November, 2020

Accepted 29th December, 2020

Published online 30th January, 2021

Key Words:

Lanthanum nitrate hexahydrate · Rare earths ·

Lanthanides · Thermal decomposition ·

Oxynitrates

*Corresponding author: Hector Marcell Guerreiro

ABSTRACT

Thermal decomposition of lanthanum nitrate hexahydrate, $\text{La}(\text{NO}_3)_3 \cdot 6\text{H}_2\text{O}$, has been studied by thermogravimetric technique, differential scanning calorimetry, infrared spectroscopy and X-ray diffractometry. At the beginning, this complex process involves slow and rapid internal hydrolysis in the liquid phase, like the processes described for the light members of the lanthanide series. In the first stage, condensation is accompanied by the removal of water to form intermediate clusters containing O-La-OH groups. No traces of lower hydrates were detected. It is assumed that the existence of intermediate compounds with six atoms of lanthanum best fits the experimental data. At higher temperatures, these products undergo further thermal degradation, releasing nitric acid, nitric acid azeotrope, nitrogen dioxide, water, and oxygen. Finally, after having lost remaining lattice water, the material is transformed into a hexagonal La_2O_3 . All mass losses are taken into account satisfactorily for under the proposed mechanism of thermal decomposition.

Copyright © 2021, Hector Marcell Guerreiro, Petr Melnikov, Igor Arkhangelsky, Lincoln Carlos Silva de Oliveira, Gabriel Augusto Wandekoken and Valter Aragão do Nascimento, 2021. This is an open access article distributed under the Creative Commons Attribution License, which permits unrestricted use, distribution, and reproduction in any medium, provided the original work is properly cited.

Citation: Hector Marcell Guerreiro, Petr Melnikov, Igor Arkhangelsky, Lincoln Carlos Silva de Oliveira, Gabriel Augusto Wandekoken and Valter Aragão do Nascimento, 2021. "Thermal decomposition of lanthanum nitrate hexahydrate $\text{La}(\text{NO}_3)_3 \cdot 6\text{H}_2\text{O}$," *International Journal of Development Research*, 11, (01), 43318-43321

INTRODUCTION

Lanthanum nitrate hexahydrate has numerous applications in the industry as precursor for the synthesis of pure lanthanum oxide, catalyst in exhaust gas converters, starting material for organic ligands used as biological spectroscopic markers, etc. (Mentus *et al.*, 2007; Cochran *et al.*, 2019). Its crystalline structure [pentaquaquateris (nitrate) lanthanum (III) hydrate] is similar to other $[\text{Ln}(\text{NO}_3)_3(\text{H}_2\text{O})_5] \cdot \text{H}_2\text{O}$ analogues. The asymmetric unit (Fig. 1)

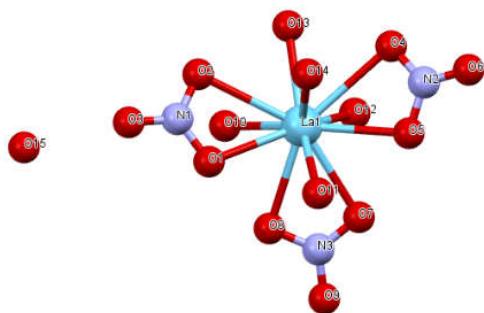


Figure 1. Structure of $\text{La}(\text{NO}_3)_3 \cdot 6\text{H}_2\text{O}$. Hydrogen atoms were not located. (Eriksson *et al.*, 1980, with modifications)

consists of a La (III) cation with CN 11 (Huang, 2010), three bidentate nitrate anions, and in total five water molecules with the distances La–O; 2.527 Å; 2.554 Å; 2.560 Å; 2.585 Å and 2.668 Å (Eriksson *et al.*, 1980). As can be seen, one lattice water molecule is located in the second coordination shell at a larger distance of 7.350 Å. This loosely bonded water may be expected to be the first to be removed during the heat treatment. The early thermo gravimetric investigations of $\text{La}(\text{NO}_3)_3 \cdot 6\text{H}_2\text{O}$ decomposition have been published in the period 1956-2007. Various mechanisms have been proposed, but there is not yet a clear understanding as for the character of intermediate products and intervals of their existence. The general idea was a stepwise dehydration with the formation of oxynitrate LaONO_3 together with the removal of N_2O_5 . Then, a condensation process would take place leading to La_2O_3 as the final product (Mentus *et al.*, 2007; Gobichon *et al.*, 1997). Unfortunately, no chemical reaction with integer stoichiometric coefficients has been proposed as a result. However, despite the expected similarities with the coordination chemistry of other nitrates, the thermal decomposition of lanthanum nitrate seems to be a more complex process due to the lower basicity of the element, therefore a different mechanism of hydrolyses may be envisaged. Continuing the previous studies (Melnikov *et al.*, 2018; 2019). this work was carried out to revert to the thermolysis of lanthanum nitrate hexahydrate to obtain a comprehensive data on the mechanisms involved, and to elaborate a more realistic scheme of its thermal transformations.

MATERIALS AND METHODS

The initial reagent used was lanthanum nitrate hexahydrate $\text{La}(\text{NO}_3)_3 \cdot 6\text{H}_2\text{O}$ of high analytical purity (99.9%), purchased from Sigma-Aldrich. The direct heating of the commercial reagent up to 800°C confirmed the presence of 6 mol of water, which resulted in a mass loss of 62.7%, so the final product must be exactly La_2O_3 (theoretical mass loss of 62.37%). The thermogravimetric analysis (TG) and differential scanning calorimetry (DSC) were used to study the thermal behavior, employing a 50H Shimadzu Instrumentation and Netsch STA Jupiter 449 C Instrumentation. The test sample of the initial reagent (7 mg) was heated in nitrogen flow (60 mL min^{-1} , 99.998% purity; oxygen content < 5 ppm), in a temperature range from room temperature up to 800°C, always at a heating rate of 5°C min^{-1} . A platinum micro receptacle was used to perform thermal treatment. Mass losses during heating were analyzed and compared with previously calculated values. Visual observations were carried out in the air, using a platinum container, from room temperature to 300°C. The evolution of volatile products was measured using a Tensor 27 Bruker FTIR spectrometer connected to the Netsch STA Jupiter 449C Instrumentation. The temperature of the transport gas line was 240°C. The IR spectra were detected in a $700 - 4000 \text{ cm}^{-1}$ range, taken for 12s at a frequency accuracy of 1 cm^{-1} . The identification was done based on NIST Chemistry WebBook (NIST, 2018).

RESULTS AND DISCUSSION

As established by visual observations, the compound melts in its own crystallization water at around 54°C . Then it starts to lose gas bubbles and turns into a clear yellow liquid. At this point, the smell of nitric acid fumes begins to be felt. At temperatures above 200°C the melt becomes viscous, and then solidifies at 260°C - 270°C , although the evolution of colorless gas continues. The subsequent heating produces brownish vapors of nitrogen dioxide. These qualitative results have represented a solid basis for a further interpretation of the experimental curves. It is well known that the decomposition onset for the nitrates of transition metals is generally below 100°C (Melnikov *et al.*, 2014) due to a back donation of electrons from the nitrate ions to an unfilled *d* orbital of the cations (Wendlandt *et al.*, 1961; Yuvarajet *et al.*, 2003). In this respect lanthanum nitrate is quite similar to other rare earth nitrates. Our working hypothesis was that $\text{La}(\text{NO}_3)_3 \cdot 6\text{H}_2\text{O}$ is hydrolyzed by the crystallization water, and as a result nitric acid should have been produced. Indeed, this acid, or rather its azeotrope, is detected by the IR sensor of the volatile products from the very beginning of the thermal treatment. Another component is nitrogen dioxide present as a product of azeotrope partial decomposition (Fig. 2).

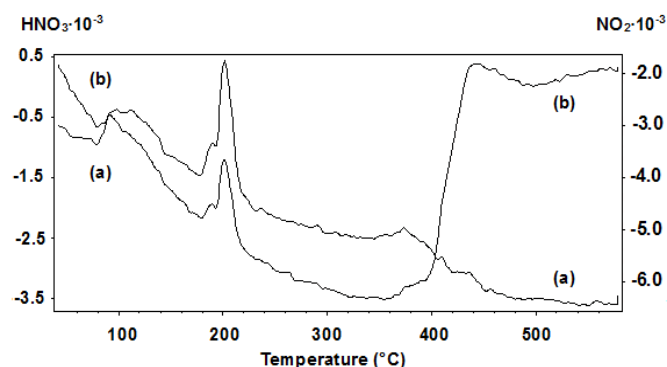


Figure 2. IR sensor data showing removal of HNO_3 (a) and NO_2 (b) at sequential temperatures

At this step, we do not have the ability to judge about precise compositions, since the mixture is in the liquid state, and the removal of HNO_3 is essentially a dynamic process. That is why direct visualization is of utmost importance. So far no such observation has

been made. Being liquid, the reactive system in this temperature range is out of equilibrium, so it is reasonable to assume that the pyrolysis curves correspond to the mixture of various chemicals, and not a set of known stoichiometric compounds. At the same time this proves the fallacy of the proposed decomposition mechanisms, which imply the sequential elimination of crystallization water. Partial dehydration may be feasible, but only when the hexahydrate is dried under low pressure for a long time (Rybar *et al.*, 1988; 1990).

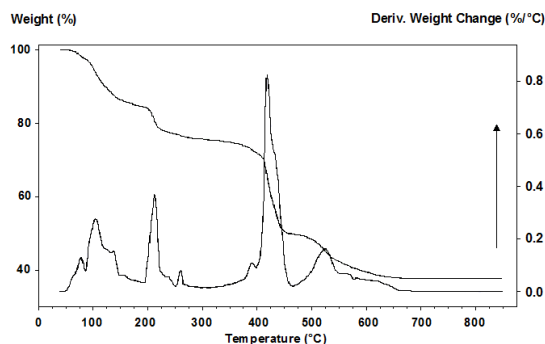


Figure 3. TG curves of $\text{La}(\text{NO}_3)_3 \cdot 6\text{H}_2\text{O}$.

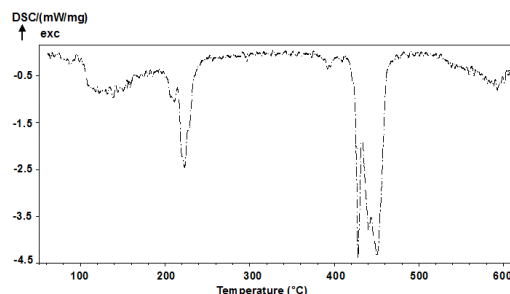


Figure 4. DSC curve of $\text{La}(\text{NO}_3)_3 \cdot 6\text{H}_2\text{O}$.

Fig.3 represents the thermogravimetric curve of $\text{La}(\text{NO}_3)_3 \cdot 6\text{H}_2\text{O}$. The corresponding DSC curve of this compound is given in Fig. 4. At lower temperatures, no phase transitions were found, at least above 40°C . From 40°C on, a series of multiple endothermic effects takes place demonstrating the complexity of dehydration/decomposition processes in the liquid and solid phases, and during their coexistence. As for mass losses, after melting in its own water of crystallization at 56°C , between 60°C and 76°C the compound loses 2.06% of mass. Between 76°C and 389°C 24.1% of mass is lost. The next loss of mass (30.0%) takes place between 389°C and 504°C . There follows a final loss of 10.2% between 504°C and 800°C . It is evident that these multiple losses cannot be produced by the disintegration of the single mol of $\text{La}(\text{NO}_3)_3 \cdot 6\text{H}_2\text{O}$, as its formula unit contains only one atom of metal, whereas at least two are needed for the formation of final La_2O_3 . Consequently, one must take into consideration the processes of condensation, characteristic of the chemistry of cations with the charge 3^+ . Here, it is worthwhile to consult the existing published data on the elements whose properties are most close to lanthanum. For neodymium, praseodymium, samarium, and dysprosium (Melnikov *et al.*, 2014; 2015; 2018; 2019), for example, it has been shown that such condensation enhances the formation of stable clusters containing six metal atoms connected via oxygen bridges. They are related to some rare earth complex nitrates $[\text{Ln}_6(\mu_6\text{-O})(\mu_3\text{-OH})_8(\text{H}_2\text{O})_{12}(\text{NO}_3)_6](\text{NO}_3)_2 \cdot x\text{H}_2\text{O}$, $\text{Ln} = \text{Y}, \text{Gd}, \text{Yb}$, $x(\text{Y}, \text{Yb}) = 4$; $x(\text{Gd}) = 5$ having a Ln_6 -nucleus (Žák *et al.*, 1994) and to europium nitrate of the composition $[\text{Eu}_6\text{O}(\text{OH})_8(\text{H}_2\text{O})_{12}(\text{NO}_3)_6](\text{NO}_3)$. These compounds were early obtained in the form of single crystals by heating of a clear solution of Ln oxide in an excess of concentrated nitric acid, until decomposition started. The melt was treated with ethyl alcohol and water, after which fine precipitates were collected (Giester *et al.*, 2009). As for the individual stages of thermal decomposition, the DTG and DCS curves can be explained as follows. At the first stage, during the process of the initial melting and dehydration of the compound and immediately afterwards, 3 mol of loosely bound water are removed. This produces a mass loss of: calc. 2.08%; exp. 2.1%. At the second stage, 15 mol of water and 6 mol of nitric acid are removed, producing a mass loss of:

calc. 24.95%; exp. 24.1%. We suggest that the internal coordination shell of lanthanum nitrate is being destroyed by a hydrolytic process, and nitric acid should have been produced as a result. Indeed, this acid, or the aforementioned azeotrope 68% HNO₃ – 32% H₂O with boiling point 120°C (Horsley, 1962) is identified by its characteristic absorption bands at 892, 1319, 1508, 1596, 1631, and 1716 cm⁻¹. The IR sensor data (Fig.2) and 3D diagram of IR spectrum (Fig. 5) give a general view of infrared absorption at sequential temperatures. In addition, they also demonstrate that at least before 390°C the release of gaseous nitric acid is completely stopped.

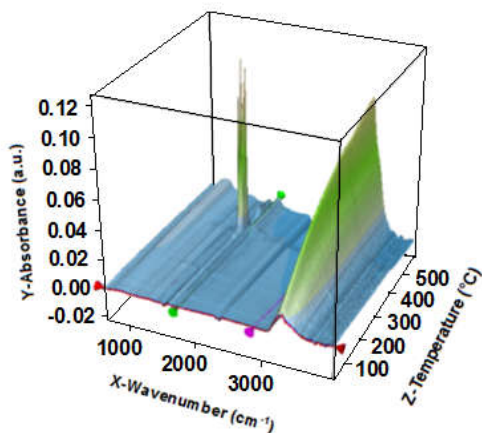


Figure 5. 3D diagram of IR spectrum at sequential temperatures

Anyway, after 220°C the liquid becomes viscous and solidifies completely at ~385°C. At the following stage nitric acid cannot be formed, so 12 mol of nitrogen dioxide and 6 mol of oxygen are removed, producing mass loss of: calc. 24.94%; exp. 25.1%. This massive release of NO₂ is confirmed by the dynamic IR spectral data (Fig.3), 3D diagram (Fig. 5), and Gram–Schmidt curve of integrated spectral IR absorbance in respect to TG and DTG curves (Fig.6). The characteristic absorbance bands at 410°C are 1.597 cm⁻¹ and 1.630 cm⁻¹ (Fig. 7). The DSC curve (Fig. 4) complements the mass loss curve showing the splitting of the main endothermic effect into minima at 413°C and 448°C. This cleavage, unnoticeable in the TG curve, may reflect the two-step disproportionation of HNO₃ at these temperatures.

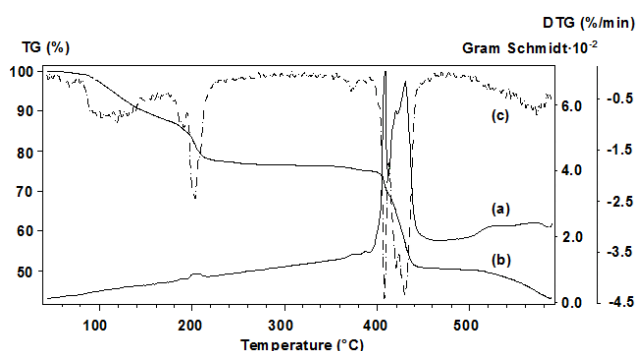


Figure 6. Gram–Schmidt curve (a) of integrated spectral IR absorbance in respect of TG and DTG curves (b, c).

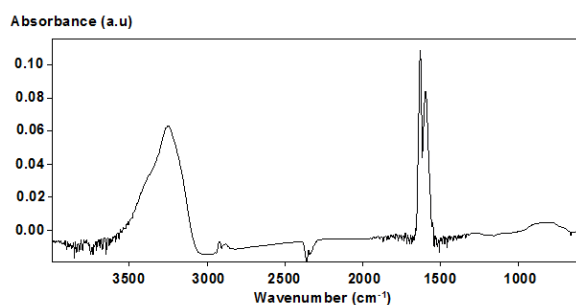
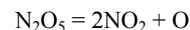
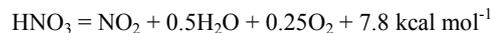


Figure 7. IR spectrum of volatile products detected at 410°C.

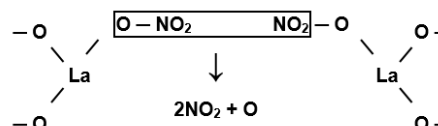
This suggests a mechanism implying the disintegration of nitrogen pentoxide into nitrogen dioxide and atomic oxygen:



Indeed, the modeling of NO_x species absorbed at high temperature gave nitrogen dioxide, water and oxygen as reaction products:



This follows from static and dynamic simulation of NO_x absorption based on a hybrid-kinetic equilibrium reaction model (Liu *et al.*, 2014). In parallel, in the solid phase, amorphous oxynitrates are being formed, which unfortunately cannot be unequivocally identified by means of IR spectra due to the overlapping bands of nitrate ion and water. Molecular modeling of the related compounds with dysprosium (Melnikov *et al.*, 2015) shows that they represent crown cycles of irregular geometry formed by six lanthanide atoms and six oxygens located in parallel planes. As the lanthanide–oxygen bonds forming the rings are preferably polar and non-covalent, the cycles have a clear tendency to be deformed. Therefore, their main feature is resistance to crystallization. The condensation occurs by releasing nitrogen pentoxide from the neighboring NO₂ groups of the initial cluster and forming intramolecular bridges O–La–O. One of these fragments is shown below:



So, at the end the elimination of the last 2NO₂ instead of metastable La₆O₁₈ will produce 3 mol of lanthanum oxide, in agreement with the X-ray pattern of the final product (Fig.8) identical to the pattern of previously characterized hexagonal La₂O₃ (PDF file 73-2141).

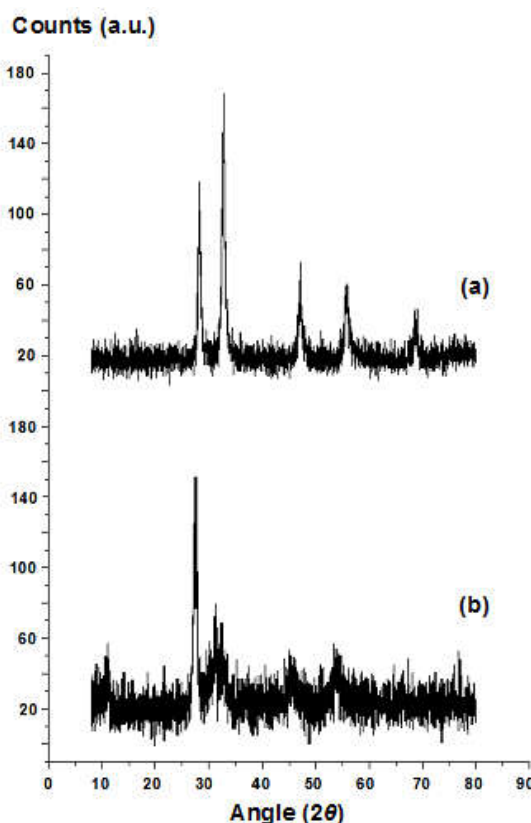


Figure 8. X-ray diffraction patterns of hexagonal La₂O₃(a) and the final product of La(NO₃)₃·6H₂O thermal decomposition (b).

As in the case of other nitrates, the peripheral water molecules are involved in intermolecular hydrogen bonding, which makes the oxide

monomers stand together. After the denitrification was completed at 530°C, the solid phase slowly loses water in two stages: between 540°C and 800°C. This corresponds to 15 mol of interstitial water and, final mass loss of calc. 9.94% and exp.10.24%. The absence of other volatile species is confirmed by the IR spectrum recorded at 530°C (Fig. 9).

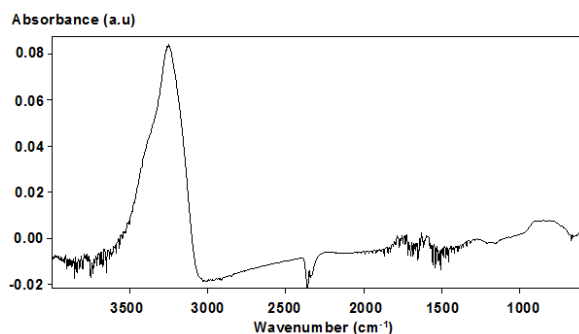


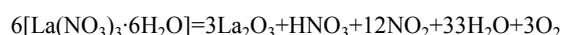
Figure 9. IR spectrum of volatile products detected at 530°C.

Table 1 provides the compositions of the volatile products along with the expected and experimentally measured mass losses.

Table 1. Mass losses (%) at different stages of $6[\text{La}(\text{NO}_3)_3 \cdot 6\text{H}_2\text{O}]$ pyrolysis and compositions of the volatile products in relation to the initial six monomers

Step	H ₂ O	HNO ₃	NO ₂	O	Exp.	Calc.
I	3				2.1	2.08
II	15	6			26.9	27.02
III	6		12	6	51.9	52.43
IV	15				56.9	58.67
3La ₂ O ₃						
Total	33	6	12	6	62.6	62.37

Calculations show that the hypothesis concerning clusters preexistence in the solid state is quite applicable to the present case of lanthanum nitrate hexahydrate. Indeed, that suggests that at least six mol of $\text{La}(\text{NO}_3)_3 \cdot 6\text{H}_2\text{O}$ are involved in the condensation process, and the decomposition can be described by the following equation:



CONCLUSION

Lanthanum nitrate hexahydrate $\text{La}(\text{NO}_3)_3 \cdot 6\text{H}_2\text{O}$ does not show mass losses or phase transitions in the range of -40°C to 54°C when it melts in its own water of crystallization. At the beginning, this complex process involves slow and rapid internal hydrolysis in the liquid phase. It is similar to the processes described for the light members of the lanthanide series. In the first stage, pyrolysis is accompanied by the removal of water to form intermediate clusters containing O-La-OH groups. No traces of lower hydrates were detected. It is assumed that the existence of intermediate compounds with six atoms of lanthanum best fits the experimental data. At higher temperatures, these products undergo further thermal degradation, releasing nitric acid, nitric acid azeotrope, nitrogen dioxide, water, and oxygen. Finally, after having lost remaining lattice water, the material is transformed into a hexagonal La_2O_3 . All mass losses are taken into account satisfactorily for under the proposed mechanism of thermal decomposition.

Acknowledgments: This study was financed by Conselho Nacional de Pesquisa (CNPq) and Coordenação de Aperfeiçoamento de Pessoal de Nível Superior-Brasil (CAPES) - Finance Code 001.

REFERENCES

- Cochran, E.A., Woods, K.N., Johnson, D.W., Page, C.J., Boettcher, S.W. 2019. Unique chemistries of metal-nitrate precursors to form metal-oxide thin films from solution: materials for electronic and energy applications. *Journal of Materials Chemistry A*. 7, pp. 24124-24149.
- Eriksson, B., Larsson, O.L., Niinistö, L., Valkonen, J. 1980. Crystal and molecular structure of the undecacoordinate complex pentaquatris(nitrato) lanthanum(III) hydrate. *Inorganic Chemistry*. 19, pp.1207-1210.
- Giester, G., Žák, Z., Unfried, P. 2009. Syntheses and crystal structures of rare earth basic nitrates hydrates: Part III. $[\text{Ln}_6(\mu_6\text{-O})(\mu_3\text{-OH})_8(\text{H}_2\text{O})_{12}(\eta^{2-}\text{NO}_3)_6](\text{NO}_3)_2 \cdot x\text{H}_2\text{O}$, Ln = Y, Sm, Eu, Gd, Tb, Dy, Ho, Er, Tm, Yb, Lu; x = 3, 4, 5, 6. *Journal of Alloys and Compounds*. 481, pp. 116-128. (and references therein).
- Gobichon, A.E., Auffrédic, J.P., Louër, D. 1997. Thermal decomposition of neutral and basic lanthanum nitrates studied with temperature-dependent powder diffraction and thermogravimetric analysis. *Solid State Ionics*. 93, pp. 51-64.
- Horsley, L.H. 1962. Azeotropic data II, *Advances in chemistry series American Chemical Society, Washington, D. C.*
- Huang, C-H. 2010. *Rare Earth Coordination Chemistry: Fundamentals and Applications*, John Wiley & Sons, Asia.
- Liu, Y., Bluck, D., Brana-Mulero, F. 2014. Static and dynamic simulation of NO_x absorption tower based on a hybrid kinetic-equilibrium reaction model. *Computer Aided Chemical Engineering*. 34, pp. 363-368.
- Melnikov, P., Arkhangelsky, I.V., Nascimento, V.A., Silva, A.F., Consolo L.Z.Z. 2014. Thermolysis mechanism of samarium nitrate hexahydrate. *Journal of Thermal Analysis and Calorimetry*. 118, pp. 1537-1541.
- Melnikov, P., Arkhangelsky, I.V., Nascimento, V.A., Silva, A.F., Consolo L.Z.Z., De Oliveira, L.C.S., Herrero, A.S. 2015. Thermolysis mechanism of dysprosium hexahydrate nitrate $\text{Dy}(\text{NO}_3)_3 \cdot 6\text{H}_2\text{O}$ and modeling of intermediate decomposition products. *Journal of Thermal Analysis and Calorimetry*. 122, pp. 571-578.
- Melnikov, P., Arkhangelsky, I.V., Nascimento, V.A., De Oliveira, L.C.S., Guimarães, W.R., Zandoni, L.Z. 2018. Thermal decomposition of praseodymium nitrate hexahydrate $\text{Pr}(\text{NO}_3)_3 \cdot 6\text{H}_2\text{O}$. *Journal of Thermal Analysis and Calorimetry*. 133, pp. 929-934.
- Melnikov, P., Arkhangelsky, I.V., Nascimento, V.A., De Oliveira, L.C.S., Wandekoken, G.A., De Albuquerque, D.M. 2019. Thermoanalytical behavior of neodymium nitrate hexahydrate $\text{Nd}(\text{NO}_3)_3 \cdot 6\text{H}_2\text{O}$. *Journal of Thermal Analysis and Calorimetry*. 139, pp. 3493-3497.
- Mentus, S., Jelić, D., Grudić, V. 2007. Lanthanum nitrate decomposition by both temperature programmed heating and citrate gel combustion. *Journal of Thermal Analysis and Calorimetry*. 90, pp.393-397. (and references therein).
- NIST Chemistry WebBook. 2018. NIST Standard Reference Database Number 69. [www.http://webbook.nist.gov/chemistry](http://webbook.nist.gov/chemistry). Accessed 13 November 2020.
- Rybar, B., Radivojevic, P., Argay, G., Kálmán, A. 1988. Structure of yttrium hydrate trihydrate. *Acta Crystallographica Section C*. 44, pp. 595-597.
- Rybar, B., Radivojevic, P., Argay, G., Kálmán, A. 1990. Structure of yttrium hydrate trihydrate. *Acta Crystallographica Section C*. 46, pp. 525-527.
- Wendlandt, W.W., Sewell, R.G. 1961. The fusion temperatures of the rare earth chloride and nitrate hydrates. *Texas Journal of Science*. 8, pp. 231-234.
- Yuvaraj, S., Fan-Yuan, L., Tsong-Huei, C., Chuin-Tih, Y. 2003. Thermal decomposition of metal nitrates in air and hydrogen environments. *Journal of Physical Chemistry B*. 107, pp. 1044-1047.
- Žák, Z., Unfried, P., Giester, G. 1994. The structures of some rare earth basic nitrates $[\text{Ln}_6(\mu_6\text{-O})(\mu_3\text{-OH})_8(\text{H}_2\text{O})_{12}(\text{NO}_3)_6](\text{NO}_3)_2 \cdot x\text{H}_2\text{O}$, Ln = Y, Gd, Yb, x(Y, Yb) = 4; x(Gd) = 5. A novel rare earth metal cluster of the M_6X_8 type with interstitial O atom. *Journal of Alloys and Compounds*. 205, pp. 235-242.
